The thermal conductivity in one-dimensional monatomic lattices with harmonic and quartic interatomic potentials

1994 J. Phys.: Condens. Matter 6 3013

(http://iopscience.iop.org/0953-8984/6/16/006)

J. Phys.: Condens. Matter 6 (1994) 3013–3024. Printed in the UK

The thermal conductivity in one-dimensional monatomic lattices with harmonic and quartic interatomic potentials

Yuuki Ohtsubo†, Norihiko Nishiguchi† and Tetsuro Sakuma‡

† Department of Engineering Science, Hokkaido Univerity, Sapporo 060, Japan

‡ Tomakomai National College of Technology, Tomakomai 059-12, Japan

Received 9 November 1993, in final form 21 January 1994

Abstract. We analyse heat transport phenomena in a one-dimensional monatomic lattice with harmonic and quartic interatomic potentials by means of the molecular dynamics technique, paying special attention to non-diffusive heat flow and local temperature profiles in steady non-equilibrium states. The non-diffusive heat current is attributed to modified KDV solitons, which decay through collisions with phonons with short wavelengths. Hence, the non-diffusive heat flow does not propagate beyond a critical distance l_{cr}. We confirm the anomalous diffusion of energy due to non-diffusive heat flow in steady non-equilibrium states for systems smaller than the critical length l_{cr}. The non-diffusive heat current does not contribute to the total heat flow for lattices larger than the critical length l_{cr}. The existence of Fourier's law is confirmed from first principles for the lattices. The temperature profiles become linear, and the resultant thermal conductivity is independent of the local temperatures of the lattice, in accordance with the temperatures profiles, so the local energy conservation law holds.

1. Introduction

Fourier's heat law is a well known phenomenological law that describes heat transport phenomena in solids, and is used in all fields of science and engineering. Although a number of numerical simulations has been performed for the derivation of Fourier's law from first principles, most attempts failed to exhibit the existence of Fourier's law since the resultant thermal conductivity depended on the system sizes [1–9]. After a series of disappointing results, Mokross and Büttner [10] suggested that a one-dimensional (1D) diatomic Toda lattice would be a candidate for normal thermal conductivity. Jackson and Mistriotis [11] investigated the heat transport in the same kinds of lattice with larger sizes than those of Mokross and Büttner, and concluded the existence of Fourier's law.

The numerical simulations for the heat transport were performed based on various postulates made so far. One of the postulates is that linear temperature profiles should appear in steady non-equilibrium states. The resultant temperature profiles became, however, often not linear but curved [8, 10, 11], but were approximated by straight lines for estimation of the thermal conductivity. The temperature profiles cannot be linear, to satisfy the local energy conservation law in the steady non-equilibrium states, where the thermal conductivity depends on local temperature. The approximation of the temperature profiles by straight lines hence discards the information on the temperature dependence of the thermal conductivity. Another postulate is that the total heat current flows diffusively. Incident energy pulses from the heat baths do not necessarily spread diffusively but propagate ballistically, as observed in some numerical experiments [8, 11]. Another example of the non-diffusive energy flow was given by Schneider and Stoll [12, 13]. They investigated

0953-8984/94/163013+12$19.50

numerically and analytically dynamical properties of 1D sine–Gordon and ϕ^4 systems, exhibiting the existence of non-diffusive energy flow due to kink solitons, which disappear at high temperatures. The non-diffusive heat flow does not obey Fourier's law, leading to an undesirable non-local property of the heat transport. Therefore the total heat current should be treated carefully for the estimation of the thermal conductivity, particularly for small systems.

The present authors [14] re-examined the heat transport in the one- and two-dimensional (2D) diatomic Toda lattices, paying special attention to the temperature profiles and to the non-diffusive heat current. The temperature profiles for both cases were well fitted with exponential functions with respect to distance from an end of the lattice, and the temperature gradient became proportional to the local temperature T accordingly. Because the heat current is constant through the lattice in the steady non-equilibrium states, the thermal conductivity was required to be inversely proportional to the local temperature T, ξ/T, where ξ is a constant. Assuming that the total heat current consisted of the non-diffusive and diffusive currents, we confirmed the existence of Fourier's law by excluding the non-diffusive or ballistically propagating heat current from the total energy flow. We also confirmed the existence of Fourier's law in 1D quasi-periodic Toda lattices [15, 16] and 2D monatomic Toda lattices [17] in the same manner.

Recently, Bourbonnais and Maynard [18] reported anomalous energy diffusion, leading to anomalous thermal conductivity, in 1D and 2D disordered lattices with very large quartic potentials. The magnitude of the quartic potentials is from 0.5 to 2^{20} times as large as that of the harmonic potentials. They examined the time evolution of spatial distribution of energy by means of the molecular dynamics technique and concluded that the energy spreading was different from the usual diffusion process. They attributed the anomaly to the delocalization of lattice-vibrational localized modes, referred to as Anderson localization [2, 19], caused by the large anharmonicity. Anderson localization is a phenomenon due to an interference effect among multiply scattered lattice-vibrational waves. The large anharmonicity significantly shortens the phase coherence length of the lattice-vibrational waves, and consequently the Anderson localization would not occur in this regime. Thus, it is hard to attribute the anomalous diffusion to the Anderson localization in strongly anharmonic lattices. Although a contribution from the non-diffusive energy flow, mainly due to the excitation of solitons, is also expected in the system, the non-diffusive energy flow has not been studied even in the case of monatomic lattices with such large anharmonicity in non-equilibrium states. The aim of this paper is to study the energy transport in a monatomic lattice with large anharmonicity and make it clear whether the system obeys Fourier's law, paying special attention to the non-diffusive energy flow.

In this paper, we investigate the heat transport in 1D monatomic lattices with harmonic and large quartic interatomic potentials, by means of the molecular dynamics technique. The plan of this paper is as follows: in section 2, we describe the model and the molecular dynamics technique for simulations. In section 3, the temperature profiles are obtained and fitted with an empirical formula. In section 4, the thermal conductivity is estimated by using the empirical formula for the temperature profiles, based on the assumption of the presence of the two different kinds of heat flow mentioned above. A summary and discussion are given in the last section.

2. Model and numerical simulations

We consider a 1D monatomic lattice with the harmonic and quartic interatomic potentials. Because direct linkage of the lattice to heat baths causes deformation of temperature profiles

in the vicinity of the interfaces due to thermal boundary resistance [20], we put monatomic Toda lattices of 10 atoms as buffer areas between the specimen lattice and the heat baths to reduce the effects of the thermal boundary resistance on the temperature profiles. The experimental situation is shown in figure 1.

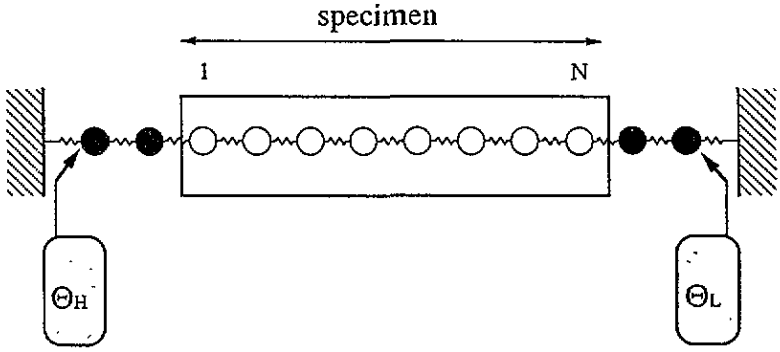

Figure 1. The model and the experimental situation for the 1D monatomic lattice. Circles denote the atoms and their masses m are set to unity in the numerical experiments. There are buffer areas at both ends of the specimen lattice in order to reduce deformation of the temperature profile due to thermal boundary resistance. The buffer areas consist of monatomic Toda lattices whose masses are also set to unity here. The lattice is heated by the elastic collisions of atoms between the lattice ends and the heat baths whose temperatures are Θ_H and Θ_L.

The total energy of the lattice is given by

$$H = \sum_{i=1}^{N'} \left\{ \frac{p_i^2}{2m} + V(u_i - u_{i-1}) \right\} + \text{interaction with heat baths} \tag{1}$$

where p_i and u_i are the momentum and displacement of the ith atom, respectively, and m denotes the atomic mass, which is set to unity in this paper. N' is the number of atoms in the lattice, and then the size of the specimen lattice N is given by $N = N' - 20$. The interatomic potential $V(r)$ in the Hamiltonian for the specimen lattice is given by

$$V(r) = \tfrac{1}{2}(ar^2 + br^4) \tag{2}$$

where r is the relative displacement. The potential parameters a and b are set to 1 and 10, respectively. The interatomic potential $V(r)$ for the buffer areas is given by the Toda potential [21] defined by

$$V(r) = \mathrm{e}^{-fr} + gr - h \tag{3}$$

where the potential parameters f, g and h are set to unity.

Energy is exchanged through elastic collisions between the end atoms and gas particles in the heat baths with prescribed temperatures Θ_H and Θ_L. The gas particles in the heat baths are assumed to obey the Maxwell distribution in velocity.

The equation of motion is integrated numerically by means of the Runge–Kutta–Gill method. The time interval is chosen suitably so that the computational errors in the total energy conservation will be suppressed within 0.1% of the total energy through the experiments.

The 1D monatomic Toda lattices are integrable, having non-linear normal modes referred to as Toda solitons. Since the Toda solitons carry ballistically all the energies without diffusion in the buffer areas, there is no temperature gradient in the buffer areas. The 1D monatomic lattices with harmonic and quartic potentials also have non-linear normal modes referred to as modified KDV (MKDV) solitons in the long-wavelength limit. On the other hand, non-diffusive normal modes with short wavelengths do not exist. Then the lattice vibrations with short wavelengths are simply expressed as phonons interacting via the quartic lattice anharmonicity, leading to irreversible behaviour of the system above a critical temperature T_{cr} [22].

At very low temperatures where lattice anharmonicity can be ignored, all vibrational excitations are phonons, which propagate ballistically in the lattice, resulting in no temperature gradient in steady non-equilibrium states. Above the critical temperature T_{cr}, the lattice vibrations with short wavelengths, which are responsible for local thermal equilibrium and for temperature gradients in non-equilibrium states, carry energy diffusively in the steady non-equilibrium states. Low-frequency lattice vibrational modes are changed from phonons to MKDV solitons. In contrast to the high-frequency phonons, the MKDV solitons may lead to undesirable non-local heat transport properties even above the critical temperature T_{cr}. It should be noted here that the ballistic propagation of the MKDV solitons will be limited due to collisions with phonons with short wavelengths in the high-temperature region because the MKDV solitons become unstable for collisions with the phonons and will propagate diffusively. Hence the normal thermal conductivity is expected for large lattices where the contribution of the MKDV solitons to heat transport is ignored.

Stochastic behaviour of the system is believed to be related to irreversibility, and divergence of trajectories starting from close points in the phase space has often been investigated quantitatively. Thereby we evaluate the Lyapunov exponent describing the rate of divergence in thermal equilibrium states. In contrast to thermal equilibrium states, the dynamical behaviour within a short time interval τ, which is characteristic of the system, is essential to the thermodynamic behaviour in the non-equilibrium states. The time interval τ is taken to be a travelling time of an energy pulse through the lattice, i.e. $\tau = N/v$, where v is the velocity of the energy pulses. Even a non-integrable system would not exhibit irreversibility with a characteristic time interval τ shorter than that τ_{cor} of the loss of correlation between initial and final positions in the phase space. How fast the correlation is lost depends on the strength of lattice anharmonicity and lattice temperature. For normal thermal conductivity, the dynamical irreversible behaviour must appear, at least, within the short time interval τ. In order to check the critical temperature T_{cr} where the dynamical behaviour of the system becomes irreversible, we investigate divergence of trajectories in the phase space in the short time interval τ. The type of divergence of trajectories is judged by the value of the quantity $\mu(\tau)$ defined by

$$\mu(\tau) = \int_0^\tau \mathrm{d}t\{|d(t) - A(q_\Gamma, p_\Gamma, \tau)\exp(k(q_\Gamma, p_\Gamma, \tau)t)|^2 - |d(t) - B(q_\Gamma, p_\Gamma, \tau)t - C(q_\Gamma, p_\Gamma, \tau)|^2\}. \tag{4}$$

Here $d(t)$ is the distance between two trajectories α and β starting in the neighbourhood of a point (q_Γ, p_Γ) in the phase space, given by

$$d(t) = \left\{ \sum_{i=1}^{N} \left[\left(q_i^{\alpha}(t) - q_i^{\beta}(t) \right)^2 + \left(p_i^{\alpha}(t) - p_i^{\beta}(t) \right)^2 \right] \right\}^{1/2}. \tag{5}$$

The distance $d(t)$ is approximated for $0 < t < \tau$ by a function of the form $A(q_\Gamma, p_\Gamma, \tau)\exp[k(q_\Gamma, p_\Gamma, \tau)t]$ and also by a linear function of the form $B(q_\Gamma, p_\Gamma, \tau)t + C(q_\Gamma, p_\Gamma, \tau)$ using the least-squares method. Here q_i^{α} and p_i^{α} denote the position and momentum, respectively, of the ith atom on the trajectory α. Therefore, negative μ denotes that the divergence of trajectories is close to exponential behaviour and, therefore, that irreversibility can be expected. We calculated the local rate of divergence 100 times at each value E/N of energy per atom. The test was performed numerically and the ratio of the number M_1 of exponential developments to the number M of total trials was obtained for the energy E/N per atom. The ratio gives the probability that the system exhibits stochastic behaviour. Figure 2 shows the resultant probability versus E/N for the lattices with N = 80, 180 and 280. Since the velocity of the pulses is 5 sites per unit time, the corresponding time intervals τ are 16, 36 and 56, respectively. The critical magnitude E_{cr}/N for the stochastic behaviour is 0.015 for N = 80 and decreases with the lattice size N. Since the energy per site is almost equal to the lattice temperature, we put the critical temperature T_{cr} as T_{cr} = 0.015 for N = 80. Then we study the heat transport in lattices larger than N = 80 above T_{cr} = 0.015 in this paper.

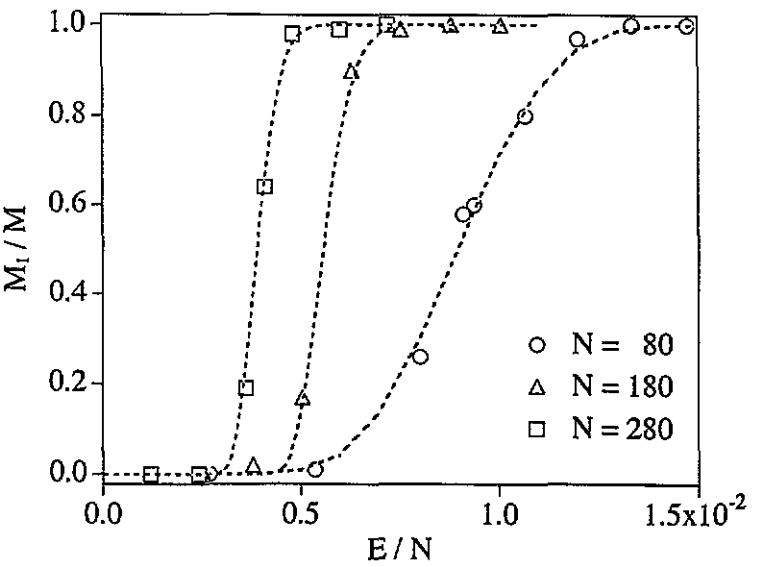

Figure 2. The probability in the phase space that the system exhibits stochastic behaviour versus the energy per atom for the monatomic lattice with the harmonic and quartic interatomic potential with N = 80, 180 and 280. The velocity of pulses v is five sites per unit time. The corresponding characteristic time interval τ is obtained by N/v as 16, 36 and 56, respectively.

3. Temperature profiles and heat current

The local temperature is defined to be twice the averaged local kinetic energy as follows:

$$T_i = 2\left\langle \frac{p_i^2}{2m} \right\rangle. \tag{6}$$

Here the angular brackets denote the time average. We obtain the temperature profiles for several temperature regions, varying the heat bath temperature whilst keeping the ratio constant, i.e. $\Theta_H/\Theta_L = 4$, through the experiments. Figure 3 shows the temperature profiles for the lattice with $N = 230$, showing linear temperature profiles over the whole temperature region. This is true for other lattices with $N = 80$, 130, 180 and 280.

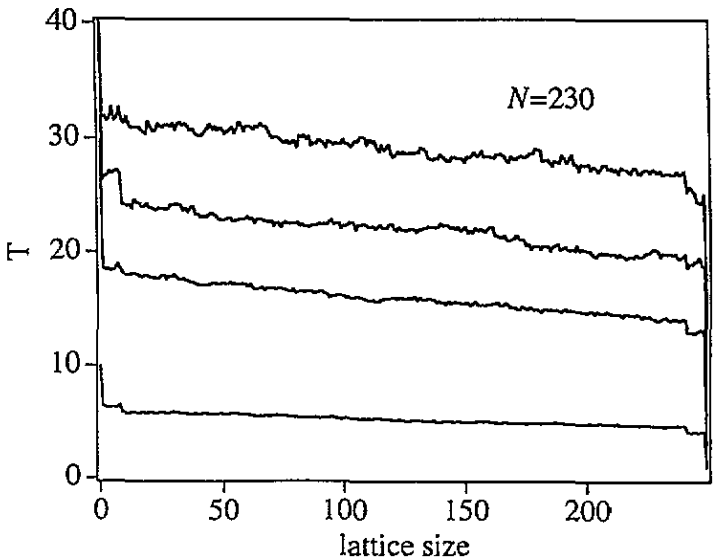

Figure 3. Temperature profiles for one-dimensional monatomic non-linear lattices. The length N of the lattices is 230 atoms. The ratios Θ_H/Θ_L of the heat bath temperatures are set to be four for all cases.

We can empirically express the temperature profiles using a linear function of the form

$$T(x) = -\frac{T_H - T_L}{N}x + T_H \tag{7}$$

where T_H and T_L are the temperatures at the ends of the specimen lattice and x measures the distance from the interface between the specimen lattice and the buffer area at the higher temperature. Here we use the notation x instead of the subscript i, for convenience. The temperature gradient is given by

$$\frac{dT(x)}{dx} = -\frac{T_H - T_L}{N}. \tag{8}$$

As mentioned in section 1, we assume that the heat current J consists of the diffusive or normal heat current J_N and the non-diffusive or ballistic heat current J_B due to MKDV solitons:

$$J = J_N + J_B. \tag{9}$$

The normal heat current J_N should obey the following Fourier law:

$$J_N = -\kappa \frac{dT}{dx} \tag{10}$$

where κ is the thermal conductivity. The normal energy flow J_N is readily found to depend on the temperature difference between the ends of the specimen lattice, by substituting (8) into (10). In contrast to the normal energy flow J_N, the non-diffusive energy flow J_B will depend on the temperature difference between the buffer areas. The MKDV solitons are excited at the interfaces between the specimen lattice and the buffer areas, the number of which increases with the temperature of the buffer areas. Then the net non-diffusive energy flow in the specimen lattice depends on the temperature difference, $T_{B,H} - T_{B,L}$, between the buffer areas. Because the MKDV solitons decay with propagating distance due to the collisions, as will be shown below, the ballistic heat current J_B is expressed as a function of the lattice size N:

$$J_B = J_B(T_{B,H} - T_{B,L}, N). \tag{11}$$

4. Thermal conductivity

Substituting equations (8), (10) and (11) into (9), we obtain an empirical formula for the heat transport in the lattice as follows:

$$J = \kappa \frac{T_H - T_L}{N} + J_B(T_{B,H} - T_{B,L}, N). \tag{12}$$

Although the heat current J and the temperatures T_H and T_L are readily known from the numerical simulations, the ballistic heat flow J_B is hard to estimate quantitatively. However, because the MKDV solitons decay with the propagating distance, due to collisions with the phonons, and will not propagate beyond a critical distance l_{cr}, we may ignore the contribution of the ballistic heat current J_B to J when $N > l_{cr}$.

In order to check the critical distance l_{cr}, we investigate the successive behaviour of a pulse excited in the lattice at a finite temperature, by using the participation ratio defined by

$$P(t) = \sum_{i=1}^{N} \frac{\langle E_i(t) \rangle^2}{\langle E_i(t)^2 \rangle} \tag{13}$$

where $E_i(t)$ is the lattice vibrational energy of the ith lattice site. The participation ratio $P(t)$ takes a value from $1/N$ to unity in accordance with the spatial distribution of the energy $\{E_i(t)\}$. When all the energies are concentrated entirely on one atom, the participation ratio

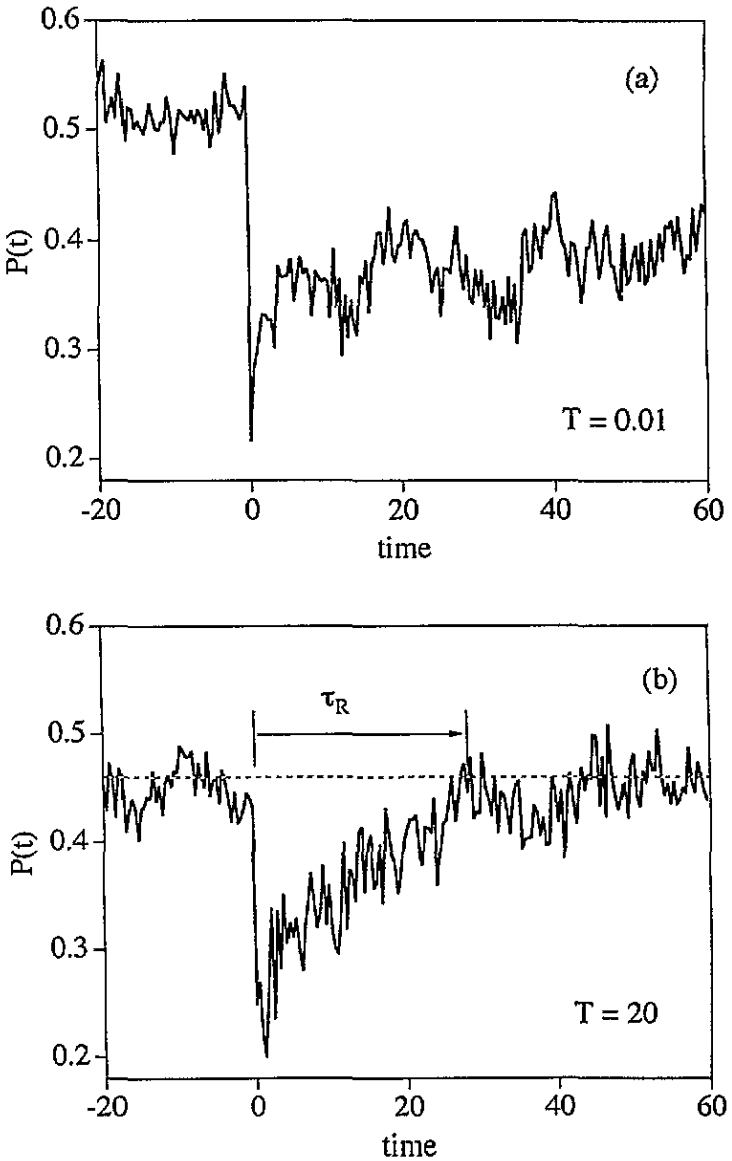

Figure 4. Participation ratios versus time at temperature $T = 0.01$ (a) and at $T = 20.0$ (b). The energy of the pulse is $E_0 = 0.20$ (a) and $E_0 = 400.0$ (b). The lattice length is 130.

$P(t)$ becomes $1/N$. On the other hand, when all the energies are shared by all of the atoms equally, $P(t)$ becomes unity.

Because the MKDV solitons propagate stably at temperatures below the critical temperature T_{cr}, the participation ratio $P(t)$ keeps a small constant value, independent of the propagating distance or time. Figure 4(a) shows the time evolution of the participation ratio $P(t)$ at temperature $T = 0.01$. A thermal equilibrium state was maintained before the excitation of the pulse. The participation ratios $P(t)$ are drastically reduced by the excitation of the pulse at $t = 0$, preserving the reduced magnitude with the propagation

distance or time. Figure 4(b) shows the participation ratio $P(t)$ versus time t at $T = 20$. The participation ratios $P(t)$ exhibit a dip at $t = 0$ due to the excitation of a pulse as in the former case at $T = 0.01$. In contrast to the previous case, the thermal equilibrium states recover quickly. The participation ratios $P(t)$ consequently increase and settle down to their magnitude at the thermal equilibrium states within a time interval τ_R. We refer to the time interval τ_R as a relaxation time hereafter. The relaxation time τ_R is 25 in the present case.

In figure 4, the energies E_0 of the pulses were set at $E_0 = 20T$. In the heat transport simulations, the heat pulses generated by the heat bath with Θ_H have energy $4.5\Theta_H$ at most, according to the three-sigma method. The temperature of the specimen lattices T is about $\Theta_H/3$–$\Theta_H/2$ from figure 2. Then the ratio E_0/T becomes of the order of 10. The relaxation time τ_R depends on the ratio E_0/T as well as the temperature T. Figure 5 shows the relaxation time τ_R versus temperature T for various values of E_0/T. The relaxation times τ_R become 30 at $T = 10$ at most, by taking account of fluctuations of the data, and decrease with increasing temperature T. The ballistic heat current J_B cannot consequently propagate over 150 sites. We may take this length as the critical propagating distance l_{cr}.

From these considerations, we estimate the thermal conductivity κ. Dividing equation (12) by the absolute temperature gradient $(T_H - T_L)/N$, we obtain

$$\frac{JN}{T_H - T_L} = \kappa + \frac{J_B(T_{B,H} - T_{B,L}, N)N}{T_H - T_L}. \tag{14}$$

Figure 6 plots $JN/(T_H - T_L)$, the heat current divided by the absolute temperature gradient, versus the temperature gradient. Apparently there is no difference between the data of the lattices with $N \geqslant 180$, which are well fitted by a straight line as shown in this figure. Although the data for the lattices with $N < 180$ also have the same magnitude as those of the lattices with $N \geqslant 180$ below $(T_H - T_L)/N = 0.02$, they increase substantially and deviate from the straight line above this region. As we discussed above, the critical length l_{cr} of the ballistic heat current is roughly 150 sites in length. Because the substantial increase of $JN/(T_H - T_L)$ is seen only for the lattices smaller than l_{cr}, we may attribute the excess of $JN/(T_H - T_L)$ over the linear dependence to the ballistic heat current J_B. At small temperature gradients, the temperature difference, $T_{B,H} - T_{B,L}$, is also small. Then the ballistic heat flow is reduced and does not contribute to the total heat current J. This is the reason why there is no difference among the data for all values of N below 0.02.

To return, we are devoted to evaluating the thermal conductivity κ. Although, according to equation (14), the magnitude of $JN/(T_H - T_L)$ should be independent of the temperature gradient for $N > l_{cr}$, the numerical data increase linearly with the absolute temperature gradient. We have assumed that the normal heat current, J_N, obeys equation (10), which is valid for small temperature gradients. For larger temperature gradients, the normal heat current J_N should be expressed in terms of the squared temperature gradient term. Therefore the heat current J_N is empirically given by

$$J_N = -\kappa \frac{dT(x)}{dx} + \beta \left[\frac{dT(x)}{dx}\right]^2 = \kappa \frac{T_H - T_L}{N} + \beta \left(\frac{T_H - T_L}{N}\right)^2. \tag{15}$$

The second term of the right hand side of equation (15) has a significant contribution to the heat flow when the temperature gradient is large. The thermal conductivity κ is defined in

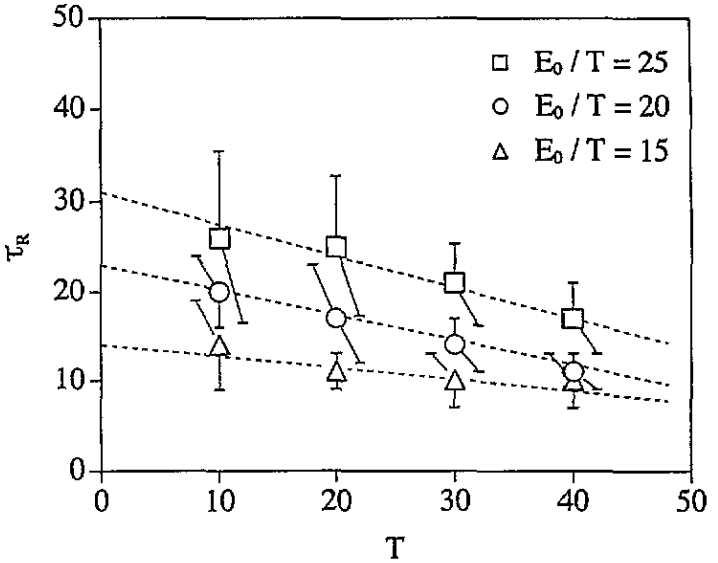

Figure 5. The relaxation time τ_R versus temperature T for E_0/T = 15, 20 and 25. The lattice length is N = 400.

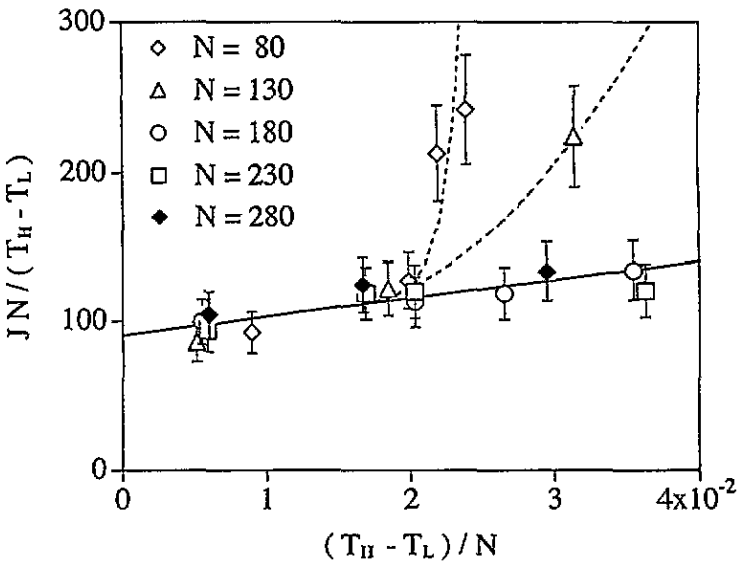

Figure 6. $JN/(T_H - T_L)$, the heat current divided by the absolute temperature gradient, versus the absolute temperature gradient $(T_H - T_L)/N$ for N = 80, 130, 180, 230 and 280. The solid line is drawn using the least-squares method for the data points with $N \geqslant 180$, to exhibit the extrapolation of the data to zero-temperature gradient. The extrapolated value of κ is 90±5. The dashed lines are drawn for the data of N = 80 and 130 by the least-squares method.

the small-temperature-gradient limit, extrapolated by taking a limit of the zero-temperature gradient

$$\kappa = \lim_{(T_H - T_L)/N \to 0} \frac{JN}{T_H - T_L}. \tag{16}$$

Thus the resultant thermal conductivity κ is obtained to be 90±5 from figure 6, independent of the lattice size N.

5. Summary and discussion

In this paper we examined the heat transport and the dynamical properties of a 1D monatomic lattice with harmonic and large quartic interatomic potentials by means of molecular dynamics.

One of the important results of this work is the confirmation of the anomalous behaviour of energy diffusion. This phenomenon is caused by the non-diffusive energy flow, which is attributed to the propagation of MKDV solitons. Because the MKDV solitons are not able to propagate beyond the critical distance l_{cr} due to collisions with thermally excited phonons with short wavelengths, the anomalous energy diffusion is observed only inside the critical region l_{cr}. This fact means that the anomalous energy diffusion is a size effect and that the macroscopic intensive quantities such as the thermal conductivity should be estimated for systems larger than the critical length l_{cr}.

Another important result is the confirmation of Fourier's law in the non-linear lattice without any mass inhomogeneity. The resultant thermal conductivity is independent of the local temperature of the lattice, so the local energy conservation law holds in the linear temperature profiles, and has a value $\kappa = 90\pm5$, independent of the lattice size.

It is surprising that the present lattices have different temperature dependence of thermal conductivity from the 1D and 2D diatomic and Fibonacci Toda lattices and 2D monatomic Toda lattices [14–17]. In real solids, the temperature dependence of thermal conductivity is independent of the type of atomic bond, but depends on the lattice structures, such as crystalline or amorphous solid structures [23]. From these facts, the temperature dependence of thermal conductivity seemed to be insensitive to types of potential function, and hence the thermal conductivity of the present lattice was expected to have the same temperature dependence as the previous cases [14–17]. However, the resultant thermal conductivity was found to be independent of the local temperature. The difference in the temperature dependence of the thermal conductivity may be closely related to the propagation and decay mechanisms of the solitary pulses in the non-linear lattices. Therefore further microscopic analysis of the energy diffusion processes is needed to investigate the origin of the temperature dependence of thermal conductivity.

In this paper we have studied the non-diffusive energy flow and its effects on energy transport phenomena in 1D lattices based on the assumption of two kinds of energy flow. The non-diffusive energy flow is not a phenomenon specific to 1D lattices but is expected in higher dimensions. Therefore we should always take account of the non-diffusive energy flow, irrespective of the dimensionality of systems, in the study of energy transport phenomena. The method used in this paper will also be useful for analysis of the energy transport phenomena in 2D or 3D systems as well as 1D lattices.

Acknowledgments

This work is supported in part by a special grant-in-aid for the promotion of education and science in Hokkaido University provided by the Ministry of Education, Science and Culture of Japan, and a grant-in-aid for scientific research from the Ministry of Education, Science and Culture of Japan (grant No 05650048).

References

[1] Payton D N, Rich M and Visscher M W 1967 *Phys. Rev.* **160** 706
[2] Matsuda H and Ishii K 1970 *Prog. Theor. Phys. Suppl.* **45** 56
[3] Nakagawa H 1970 *Prog. Theor. Phys. Suppl.* **45** 23
[4] Rich M and Visscher W M 1975 *Phys. Rev.* B **11** 2164
[5] MacDonald R A and Tsai D H 1978 *Phys. Rep.* **46** 1
[6] Toda M 1979 *Phys. Scr.* **20** 424
[7] Mountain R D and MacDonald R A 1983 *Phys. Rev.* B **28** 3022
[8] Mareschal M and Amellal A 1988 *Phys. Rev.* A **37** 2189
[9] Visscher W M 1976 *Methods Comput. Phys.* **15** 371
[10] Mokross F and Büttner H 1983 *J. Phys. C: Solid State Phys.* **16** 4539
[11] Jackson E A and Mistriotis A D 1989 *J. Phys.: Condens. Matter* **1** 1223
[12] Schneider T and Stoll E 1978 *Phys. Rev.* B **17** 1302
[13] Schneider T and Stoll E 1981 *Phys. Rev.* B **23** 4631
[14] Nishiguchi N and Sakuma T 1990 *J. Phys.: Condens. Matter* **2** 7575; 1991 *J. Phys.: Condens. Matter* **3** 10077
[15] Nishiguchi N, Takahashi N and Sakuma T 1992 *J. Phys.: Condens. Matter* **4** 1465
[16] Nishiguchi N, Takahashi N and Sakuma T 1992 *Japan. J. Appl. Phys. Suppl.* **31** 179
[17] Nishiguchi N, Kawada Y and Sakuma T 1992 *J. Phys.: Condens. Matter* **4** 10227
[18] Bourbonnais R and Maynard R 1990 *Phys. Rev. Lett.* **64** 1397
[19] Anderson P W 1958 *Phys. Rev.* **109** 1492
[20] Khalatnikov I M 1952 *Zh. Eksp. Teor. Fiz.* **22** 687; 1965 *Introduction to the Theory of Superfluidity* (New York: Benjamin) ch 23 p 138
[21] Toda M 1967 *J. Phys. Soc. Japan* **22** 431
[22] Fermi E, Pasta J and Ulam S 1955 *Los Alamos Report* LA-1940
[23] Carruthers P 1961 *Rev. Mod. Phys.* **33** 92